19th Brazilian Congress of Thermal Sciences and Engineering
November 6th–10th, 2022, Bento Gonçalves - RS - Brazil

ENC-2022-0720
STABILIZED FINITE ELEMENT METHOD ON THE FLOW OF YIELD STRESS FLUIDS

Natan A. de Oliveira
Guilherme H. Fiorot
Sérgio L. Frey
Federal University of Rio Grande do Sul, Sarmento Leite 425, Porto Alegre, RS 90050-170, Brazil
natan.oliveira@mecanica.ufrgs.br; guilherme.fiorot@ufrgs.br; frey@mecanica.ufrgs.br

Abstract. *Elasto-viscoplastic materials are applied in several significant applications. The viscoplastic behavior is associated with a yield stress limit that allows the presence of unyielded regions on the flow, where the stress became less than the material yield stress and the material does not flow creating unyielded regions. This work addresses numerical simulations considering the external flow of an elasto-viscoplastic material around an immerse blade. The mechanical model is made-up of the usual mass and momentum balance equations for incompressible, inertial, and steady flows. The Oldroyd-B viscoelastic equation coupled with a transport equation for the material microstructure is considered to allow elasticity, shear-thinning, and yield stress behavior. The model is approximated by a three-field stabilized Galerkin least-squares variational method, in terms of pressure, velocity and extra-stress, via bilinear finite elements. Preliminary numerical simulations are focused on the influence of inertia on the morphology of unyielded regions over the blade of an elasto-viscoplastic material.*

Keywords: *elasto-viscoplastic; FEM; immerse blade; microstructure; yield-stress materials*

1. INTRODUCTION

Elasto-viscoplastic fluids are structured materials that exhibit complex non-Newtonian behavior related to their structure state, which in turn depends on the level of stress applied to it. Below a certain stress threshold called yield stress, the material is highly structured, with high elasticity and viscosity levels. This region can be called the apparent unyielded region. When submitted to stress levels above the yield value, the material experiences a structure break-up leading to a fluid-like behavior where viscosity decays orders of magnitude, and elasticity tends to disappear. This class of materials is present in several important industrial sectors, such as oil, food, pharmaceutical, and cosmetics. Therefore, modeling its complex non-linear mechanical behavior is of extreme industrial relevance for predicting and understanding the different processes they are subjected to.

Regarding the characterization of viscoelastic fluids and their dependence on the fluid microstructure, Acierno *et al.* (1976) presented the first considerations when referring to the dependence of rheological variables and the structure of the material based on network theory considerations. These considerations led to the concept of what were previously considered constants of rheological variables, particularly the relaxation time. The prediction of the effects associated with the viscoelastic behavior ensures the physical character of the proposed model. Unlike previous models that consider local kinematic quantities, in relation to space and time, the proposed model considers the kinematic history. This pioneering study set a precedent for disseminating the model in later publications.

de Souza Mendes (2011) presented a model of elasto-viscoplastic fluids allowing the viscoelasticity, yield stress characteristics and others non-linear effects, and through the introduction of terms related to fluid microstructure, the characterization of time-dependent fluids as the class of thixotropic and rheopectic fluids. The model called thixotropic elasto-viscoplastic considers an evolution equation relating transport terms and the construction and destruction of the fluid microstructure as a function of kinematic variables.

de Souza Mendes and Thompson (2012) showed the dependence of contemporary models to describe the time-dependent behavior, specifically with thixotropic fluids, through microstructure evolution equations. The classification of models in terms of formulation makes it possible to understand the need for formulation based on differential systems based on viscoelastic formulation. Formulations of this nature allow the characterization of viscoelastic and thixotropic behavior.

Fonseca *et al.* (2013) presented the approximate numerical solution of the formulation of elasto-viscoplastic fluids with thixotropic behavior decretized by the stabilized Galerkin least-squared method. The pioneering study in obtaining a two-dimensional numerical solution for this class of fluids considered the influence of rheological parameters on the flow topology. Fluid microstructure and non-flowing regions are inversely related to fluid microstructure equilibrium time, a parameter that describes the thixotropic nature of the fluid in regions with high strain rates.

Analogously to the study of Fonseca *et al.* (2013), but considering a different geometry, Link *et al.* (2015) presented the numerical solution of thixotropic elasto-viscoplastic fluids through the stabilized GLS methods considered the influence of the fluid microstructure equilibrium time and the strain response time on the topology of rheological variables such as unyielded regions and fluid structuring level. The results obtained describe the relationship between the fluid microstructure equilibrium time and the material microstructure. The fluid deformation response time influences both the dispersion of unyielded regions and the fluid microstructure.

Oishi *et al.* (2016) presented the transient solution of the thixotropic elasto-viscoplastic fluid using the finite difference method. The study considered the surface deformation and the action of gravitational acceleration in the destruction of the fluid microstructure. The dimensionless relaxation time and the microstructure equilibrium time are related to the fluid microstructure destruction process. The fluid response time to deformation is related to the surface deformation of the fluid. For the authour the fluid response time to deformation is related to the maximum Cauchy stress and the material elastic modulus for the fully structured fluid. This manipulation makes it possible to generalize the material response and observe the response to fluid deformation by the action of field forces and the response of the fluid microstructure to deformation.

In this work, we obtain the numerical solution of the governing conservation equations using a three-field Galerkin least-squares finite element formulation Behr *et al.* (1993a) which takes into account velocity, pressure and extra-stress fields as primal variables. Due to the addition of mesh-dependent terms to the governing equations to the Galerkin method, the formulation is capable of capturing elasto- and advective-dominated flow regions, even using equal-order finite elements. Computations investigate the elasticity and inertia influences on the elasto-viscoplastic flow pattern.

2. MECHANICAL MODEL

Considering a fluid domain $\Omega \in \Re^2$ with regular boundaries Γ where variables are prescribed Γ_g and fluxes are imposed Γ_h with $\Gamma = \Gamma_h \cup \Gamma_g$. The governing equations that describes the flow of viscoelastic materials is given by:

$$\partial_{x_i} u_i = 0, \quad \text{at} \quad \Omega \tag{1}$$

$$\rho u_j(\partial_{x_j} u_i) = \partial_{x_i} p + \eta_s \partial_{x_j} \dot{\gamma}_{ij} + \partial_{x_j} \tau_{ij}, \quad \text{for} \quad \mathrm{i} = 1, .., \mathrm{N} \quad \text{at} \quad \Omega \tag{2}$$

$$\tau_{ij} + \theta_1(\lambda) \check{\tau}_{ij} = \eta_s(\lambda)\, \dot{\gamma}_{ij}, \quad \text{for} \quad \mathrm{i,j} = 1, ..., \mathrm{N} \quad \text{at} \quad \Omega \tag{3}$$

where u_i is the velocity field, ρ is the fluid density, p is the mean pressure, and η_∞ is the solvent viscosity. The tensor $\dot{\gamma}_{ij} = (\partial_{x_j} u_i + \partial_{x_i} u_j)$ and τ_{ij} is the rate of strain and extra-stress, respectively, and $\check{\tau}_{ij} = \partial_t \tau_{ij} + u_k(\partial_{x_k} \tau_{ij}) - (\partial_{x_k} u_i)\tau_{ij} - (\partial_{x_i} u_k)\tau_{ij}$ is the upper-convected extra-stress. Momentum and Oldroyd-B–like constitutive equation, Eq. (2) - (3), are resultant from the EVSS (Rajagopalan *et al.*, 1990).

2.1 Structured behavior

The structured elasto-viscoplastic (EVP) material is a special case of the structured thixotropic elasto-viscoplastic (TEVP) as proposed by (Mendes, 2011). A structured material is composed by a polymer portion, characterized by the microstructural level, and a Newtonian solvent portion. The polymer behavior is characterized by the microstructure level λ, a dimensionless quantity that ranges from 0, for a fully-unstructured material, to 1, for a fully-structured material. The microstructure level is submitted to a transport equation given by:

$$D_t\lambda = \frac{1}{t_{eq}} \left[(1-\lambda)^a - (1-\lambda_{eq}(\tau'))^a \left(\frac{\lambda}{\lambda_{eq}(\tau')} \right)^b \left(\frac{\tau'}{\eta_s(\lambda)\dot{\gamma}} \right)^c \right], \quad \text{at} \quad \Omega \tag{4}$$

where $D_t\lambda$ is the material derivative of the microstructure $\partial_t\lambda + u_j(\partial_{x_j}\lambda)$, that account the rate of variation of λ, and the advective variation of λ. The t_{eq} is the equilibrium time of the microstructure, that characterize the thixotropic behavior of the microstructure. The first term right-hand side, $(1-\lambda)^a$ is the microstructure break-up term, and $(1-\lambda_{eq}(\tau'))^a \left(\frac{\lambda}{\lambda_{eq}(\tau')} \right)^b \left(\frac{\tau'}{\eta_s(\lambda)\dot{\gamma}} \right)^c$ is the breakdown term, and a, b, and c are dimensionless positive constants.

The build-up and breakdown terms are related to the response of the fluid to the stress level. The is introduced in the microstructure stress $\eta_s(\lambda)\dot{\gamma}$ and deviatoric stress $\tau'_{ij} = \tau_{ij} + \frac{1}{3}(\mathrm{tr}\,\tau_{ij})1_{ij}$. Where $\eta_s(\lambda)$ is the microstructure viscosity as seen ahead, $\dot{\gamma} = \sqrt{\frac{1}{2}\,\mathrm{tr}\,\dot{\gamma}^2_{\mathrm{ij}}}$ is the rate of strain intensity and $\tau' = \sqrt{\frac{1}{2}\,\mathrm{tr}\left[(\tau_{\mathrm{ij}} + \frac{1}{3}\,(\mathrm{tr}\,\tau_{\mathrm{ij}})\,1_{\mathrm{ij}})^2\right]}$ is the deviatoric stress intensity. The microstructure level is dependent on the deriatoric stress intensity. The material microstructure is only

break by the cross components of the extra-stress tensor (Mendes, 2011). At steady state $\partial_t \lambda = 0$, the equilibrium microstructure $\lambda_{eq}(\tau') \equiv \lambda_{eq}(\dot{\gamma})$ is given by:

$$\lambda_{eq}(\dot{\gamma}) = \frac{\ln \eta_{eq}(\dot{\gamma}) - \ln \eta_\infty}{\ln \eta_0 - \ln \eta_\infty} \tag{5}$$

where η_0 and η_∞ are the viscosity at zero- and infinity-rate of strain intensity (fully-structured and fully-unstructured level, respectively). And $\eta_{eq}(\dot{\gamma})$ is the equilibrium viscosity with the rate of strain intensity given by:

$$\eta_{eq}(\dot{\gamma}) = \left\{1 - \exp\left(-\frac{\eta_0 \dot{\gamma}}{\tau_0}\right)\right\}\left[\frac{\tau_0}{\dot{\gamma}} + K\dot{\gamma}^{n-1} + \eta_\infty\right] \tag{6}$$

where τ_0 is the yield-stress. Eq. (6) is the regularized *de Souza Mendes* (SMD) yield-stress viscoplastic function (Mendes and Dutra, 2004). This model has four well-fitted transition regions described by:

$$\dot{\gamma}_1 \equiv \frac{\tau_0}{\eta_0} \quad ; \quad \dot{\gamma}_2 \equiv \left(\frac{\tau_0}{K}\right)^{1/n} \quad ; \quad \dot{\gamma}_2 \equiv \left(\frac{K}{\eta_\infty}\right)^{1/(1-n)} \tag{7}$$

for $\dot{\gamma} > \dot{\gamma}_0$, the fluid has a Newtonian plateau with $\eta_{eq}(\dot{\gamma}) = \eta_0$; for $\dot{\gamma}_0 \geq \dot{\gamma} > \dot{\gamma}_1$, the fluid has a linear behavior (as in Bingham function); for $\dot{\gamma}_1 \geq \dot{\gamma} > \dot{\gamma}_2$, the fluid has a power-law behavior (as in the Herschel-Bulkley function); and for $\dot{\gamma} \geq \dot{\gamma}_2$, the Newtonian plateau is recovered with $\eta_{eq}(\dot{\gamma}) \equiv \eta_\infty$, as seen in Fig. (1). The SMD function is well-fitted for a wide range of rate of strain and represents with precision the fluid resistance to flow.

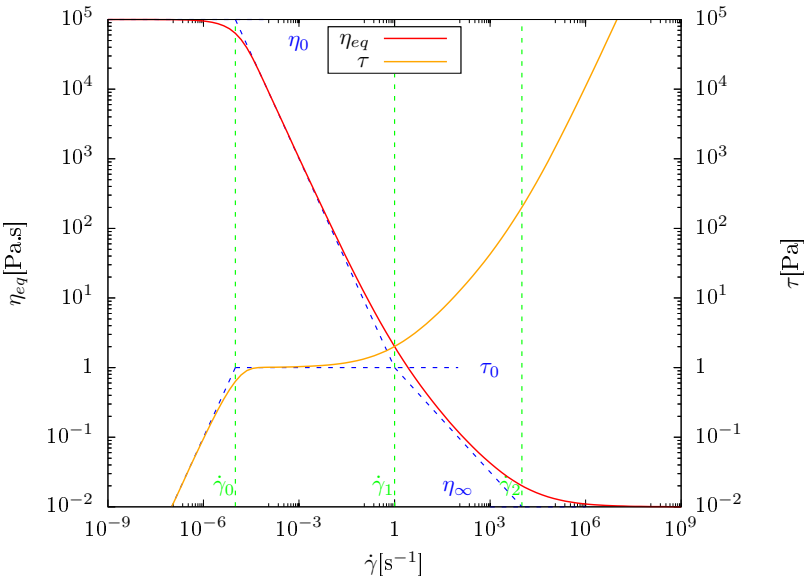

Figure 1: Flow and viscosity curve for yielded material SMD function.

From Eq. (3), the structured relaxation time $\theta_1(\lambda)$ is given by:

$$\theta_1(\lambda) = \left(1 - \frac{\eta_\infty}{\eta_s(\lambda)}\right)\frac{\eta_s(\lambda)}{G_s(\lambda)} \tag{8}$$

where $G_s(\lambda)$ is the structured elastic modulus given by, Eq. (9). The limit case $\eta_\infty \to 0$ $\theta_1(\lambda) = \eta_s(\lambda)/G_s(\lambda)$. And for $\theta_1(\lambda \to 1) = \eta_0/G_0 = \theta_0$, where G_0 is the fully-structured elastic modulus.

$$G_s(\lambda) = G_0 \exp\left[m\left(\frac{1}{\lambda} - 1\right)\right] \tag{9}$$

where m is a dimensionless positive constant that evaluate the sensitivity level of the elastic modulus, studied below. The microstructural viscosity, Eq. (3), is given by:

$$\eta_s(\lambda) = \eta_\infty\left(\frac{\eta_0}{\eta_\infty}\right)^\lambda \tag{10}$$

For the present flow, t_{eq} is set equal to zero, and Eq. (4) is reduced to $u_j(\partial_{x_j}\lambda) = 0$. If the equilibrium time is zero, the thixotropic behavior is neglected but the microstructure of the material is mainteined.

3. NUMERICAL METHOD

The approximated solution of the flow of structured elasto-viscoplastic material is obtained via a stabilized Galerkin least-square method for three primal variables - velocity, pressure and extra-stress. The stabilized GLS method is based in the finite element subsets:

$$\begin{aligned}
\Sigma_{ij}^h &= \{S_{ij}^h \in \mathcal{C}^0(\Omega) \cap L_2,\, \forall\, i,j = 1,...,N \mid S_{ij}^h|_K \in P_k(K),\, \forall\, K \in \Omega^h\} \\
\mathcal{V}_i^h{}_g &= \{v_i^h{}_g \in H_1(\Omega),\, \forall\, i = 1,...,N \mid v_i^h{}_g|_K \in P_n(K),\, \forall\, K \in \Omega^h\} \\
\mathcal{V}_i^h &= \{v_i^h \in v_i^h = 0,\, \forall\, i = 1,...,N \mid v_i^h|_K \in P_n(K),\, \forall\, K \in \Omega^h\} \\
P^h &= \{q^h \in \mathcal{C}^0(\Omega) \cap L_2^0 \mid q^h|_K \in P_m(K),\, \forall\, K \in \Omega^h\}
\end{aligned}$$

where $\mathcal{C}^0$ is the continuous space function, L_2 is the square integrable Hilbert space function,H_1 is the integrable first derivative Sobolev space function:

$$\begin{aligned}
L_2(\Omega) &= \{q^h \mid \int_\Omega (q^h)^2\, d\Omega < \infty\} \\
L_2^0(\Omega) &= \{q^h \in L_2(\Omega) \mid \int_\infty q^h\, d\Omega\} \\
H_1(\Omega) &= \{v_i \in L_2(\Omega),\, \forall\, i = 1,...,N \mid \partial_{x_j} v_i \in L_2(\Omega),\, \forall\, i = 1,...,N\} \\
H_1^0(\Omega) &= \{v_i \in H_1(\Omega),\, \forall\, i = 1,...,N \mid v_i = 0,\, \forall\, i = 1,...,N \,\text{at}\, \Gamma_g\}
\end{aligned}$$

From Eq. (1) - (4), the three-field stabilized GLS formulation is given as follow: Given: $u_i^g : \Gamma_g \to \Re$, $\tau_{ij}^h : \Gamma_h^{\tau_{ij}} \to \Re$, and $t_i : \Gamma_h^{t_i} \to \Re$. Find the triple: $(\tau_{ij}^h, u_i^h, p^h) \in (\Sigma_{ij}^h \,\mathrm{x}\, \mathcal{V}_i^h \,\mathrm{x}\, P^h)$ that satisfies the relation:

$$\mathcal{B}(\tau_{ij}^h, u_i^h, p_h; S_{ij}^h, v_i^h, q^h) = \mathcal{F}(S_{ij}^h, v_i^h, q^h), \quad \forall \quad (S_{ij}^h, v_i^h, q^h) \in (\Sigma_{ij}^h \,\mathrm{x}\, \mathcal{V}_i^h \,\mathrm{x}\, P^h) \tag{11}$$

where $\mathcal{B}(\cdot,\cdot)$ is the bilinear form and $\mathcal{F}(\cdot)$ is the linear form, as follow:

$$\begin{aligned}
\mathcal{B}(\tau_{ij}^h, u_i^h, p_h; S_{ij}^h, v_i^h, q^h) &= \langle \tau_{ij}^h, S_{ij}^h \rangle + \langle \theta_s(\lambda) \check{\tau}_{ij}^h \rangle - \langle \eta_s(\lambda) \dot{\gamma}_{ij}^{u^h}, S_{ij}^h \rangle - \langle \rho u_j^h, \partial_{x_j} v_i^h \rangle \\
-\langle p^h, \partial_{x_i} v_i^h \rangle + \langle \tau_{ij}^h, \dot{\gamma}_{ij}^{v^h} \rangle + \langle \eta_\infty \dot{\gamma}_{ij}^{u^h}, S_{ij}^h \rangle + \langle \partial_{x_i} u_i^h, q^h \rangle + \delta(Re_K) \langle \partial_{x_i} u_i^h, \partial_{x_i} v_i^h \rangle \\
+ \sum_{K \in \Omega^h} \alpha(Re_K) \langle (\rho u_j^h \partial_{x_j} u_i^h + \partial_{x_i} p^h - \partial_{x_j} \tau_{ij}^h - \eta_\infty \partial_{x_j} \dot{\gamma}_{ij}^{u^h}) \\
(\rho u_j^h \partial_{x_j} v_i^h + \partial_{x_i} q^h - \partial_{x_j} S_{ij}^h - \eta_\infty \partial_{x_j} \dot{\gamma}_{ij}^{v^h}) \rangle \\
+\beta \, \langle (\tau_{ij}^h + \theta_s(\lambda) \check{\tau}_{ij}^h - \eta_s(\lambda) \dot{\gamma}_{ij}^{u^h}), (S_{ij}^h + \theta_s(\lambda) \check{S_{ij}^h} - 2\, \eta_\infty \dot{\gamma}_{ij}^{v^h}) \rangle
\end{aligned} \tag{12}$$

where $\dot{\gamma}_{ij}^{u^h} = (\partial_{x_j} u_i^h + \partial_{x_i} u_j^h)$ and $\dot{\gamma}_{ij}^{v^h} = (\partial_{x_j} v_i^h + \partial_{x_i} v_j^h)$ is the approximated velocity rate of strain tensor and the variational velocity rate of strain. *And:*

$$\mathcal{F}(S_{ij}^h, v_i^h, q^h) = \langle t_i, v_i^h \rangle \,|_{\Gamma_h} \tag{13}$$

where $\delta(Re_K)$ and $\alpha(Re_K)$ are stability parameters mesh dependent of the continuity and momentum equations, and β is a constant stability parameter of the constitutive equation. The formulation based in the extra-stress, velocity and pressure three-field stabilized GLS formulation is proposed by (Behr *et al.*, 1993b). The formulation base in the same three primal variables stabilized GLS formulation for the Oldroyd-B viscoelastic constitutive equation is proposed by (Behr *et al.*, 2004).

3.1 Non-linear problem

The resulting non-linear system of equations, Eq. (12) and (13), is solved by a quasi-Newton's method that makes use of a frozen Jacobian gradient strategy (Zinani and Frey, 2006). All computations are accepted to be accurate when the residual of the quasi-Newton algorithm is equal to $1\mathrm{E}{-}07$.

Since the material non-linearity grows drastically for increasingly values of the relaxation time, a zero-order continuation strategy over the elastic term of Oldroyd-B constitutive model is implemented – that allows convergence even in high elasto-dominated flows. In spite of the flow intensity increase did not prove to be so troublesome, a continuation scheme on incremental velocity is also used in order to speed up convergen of flows subjected to high levels of flow intensity.

4. COMPUTATIONAL FEATURES

4.1 Domain and boundary conditions

This work geometry is a blade immerse in a structured elasto-viscoplastic material. The blade with lenght l, negligible height, and infinity width is immersed in retangle a with total lenght $L + l = 101\,l$, where $L = 100\,l$, height $H = 25\,l$, and infinity width, as seen Fig. (2). The blade is positioned in the origin of coordinate system. The coordinate Cartesian system is oriented at the beginning of the blade and the flow is dominant in the positive direction of x_1-direction. The proposed domain is a x_1 and x_2 plane. The x_3-direction effects are neglected.

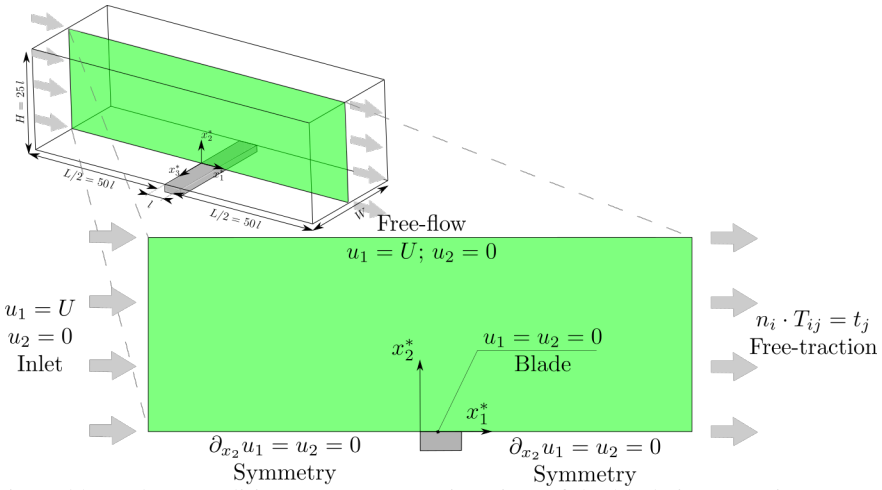

Figure 2: Domain and boundary conditions: a representative view of the blade immerse in a EVP fluid.

On the blade, no-splip ($u_1 = 0$) and impermeability ($u_2 = 0$) conditions are imposed. In the symmetry plane, shear-stress ($\partial_{x_2} u_1 = 0$) and impermeability conditions are imposed. In the inlet, a velocity vector ($u_1 = U$ and $u_2 = 0$) is imposed. On the domain's top, a free-flow boundary, the same inlet velocity vector is considered. And in the outlet, a free-traction ($n_i \cdot T_{ij} = t_j$) is imposed.

4.2 Equilibrium values

Differently to the structured TEVP model, where $\partial_t \lambda \neq 0$ and build-up and breakdown terms are present, the structured EVP model achieve the equilibrium rate of strain $\dot{\gamma}_{eq}$ instantaneously after the stress.

The procedure to achieve $\dot{\gamma}_e$ is, see Fig. (3): for a given stress intensity τ, the implicit transcedental function $\dot{\gamma}_{eq} = \tau/\eta_{eq}(\dot{\gamma}_{eq})$ is solved iteratively by the Newton's method, where $\eta_{eq}(\dot{\gamma}_{eq})$ is the SMD viscosity function, Eq. (6).

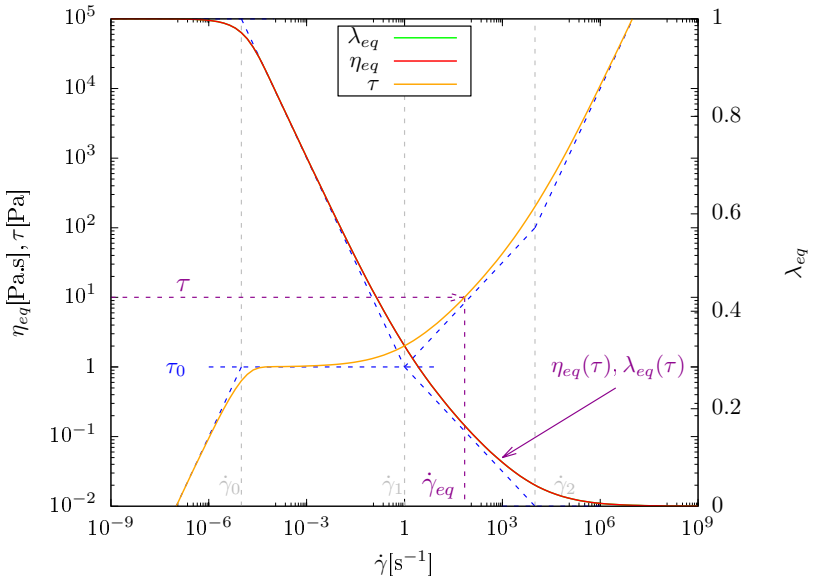

Figure 3: Equilibrium values of *de Souza Mendes* viscosity function, microstructure parameter, and extra-stress.

Then, $\dot{\gamma}_{eq}$ is evaluated to satisfies the equilibrium viscosity in terms of stress $\eta_{eq}(\tau) = \tau/\dot{\gamma}_{eq}$. Once $\dot{\gamma}_{eq}$ converge, it is solved the equilibrium SMD viscosity function and the equilibrium microstructure parameter, Eq. (5), and the iterative procedure goes forward to a new step of the solution until the convergence.

5. RESULTS AND DISCUSSION

5.1 Governing parameters

The dimensionless formulation of the governing equations are made-up based in the kinematical. Besides the rheological dimensionless formulation, see (Mendes, 2007), for this type of problem, the kinematical formulation is based only in parameters related to the flow. Considering the following dimensionless variables of the problem:

$$t^* \equiv t\dot{\gamma}_c \quad ; \quad u^*_{ij} \equiv \frac{u_{ij}}{\dot{\gamma}_c L} \quad ; \quad p^* \equiv \frac{p}{\eta_c \dot{\gamma}_c} \quad ; \quad \tau^*_{ij} \equiv \frac{\tau_{ij}}{\eta_c \dot{\gamma}_c} \quad ; \quad \dot{\gamma}^*_{ij} = \frac{\dot{\gamma}_{ij}}{\dot{\gamma}_c} \tag{14}$$

where $\dot{\gamma}_c$ is a characteristic rate of strain, L is a characteristic lenght, and η_c is a characteristic viscosity. The dimensionless form extends to the intensity of the tensors.

The kinematical dimensionless form relates the characteristic dimensions of the problem with flow quantities or related with. The characteristic variables, Eq. (14), are described as: $\dot{\gamma}_c = U_\infty/l$, the characteristic viscosity $\eta(\dot{\gamma}_c) = K(U_\infty/l)^{(n-1)}$, and characteristic lenght l. Where U_∞ is the free flow velocity. From the Eq. (1) - (10), give rise the kinematical dimensionless governing parameters:

$$HB \equiv \frac{\tau_0}{K}\left(\frac{L}{U_\infty}\right)^n \quad ; \quad Re_{PL} \equiv \frac{\rho U_\infty^{2-n} l^n}{K} \quad ; \quad Wi \equiv \theta_0\left(\frac{U_\infty}{l}\right)$$
$$Pa \equiv \frac{U_\infty}{\dot{\gamma}_0\, l} \quad ; \quad \eta^*_\infty = \left(\frac{\dot{\gamma}_2\, l}{U_\infty}\right)^{n-1} \quad ; \quad K^* = 1$$

where HB is the Herschel-Bulkley number equivalent with the Bingham number (yield-stress sensitivity to flow intensity), Re_{PL} is the power-law Reynolds number, Wi is the Weissenberg number, Pa is the Papanastasious number, η^*_∞ is the dimensionless infinity viscosity, and K^* is the dimensionless consistency index.

5.2 Sensibility analysis

The sensibility analysis is performed in both longitudinal (x^*_1) and transversal (x^*_2) direction. The domain is discretized in three regions: inlet, outlet, and blade region, as seen in Fig. (4). The inlet and outlet regions have equal number of nodes in each mesh refinement. The mesh is a combination of equal and low-order bi-linear Lagrangian finite element for both

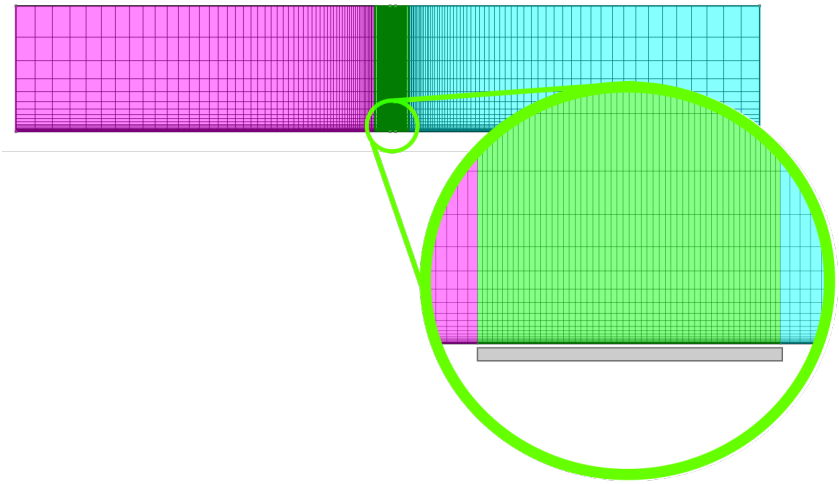

Figure 4: Domain detail. *Inlet, outlet, and plate regions are colored in pink, blue, and green respectively.*

primal variables ($Q2/Q2/Q2$). The stabilized method allow the use of this type of finite element ensuring convergence but no accuracy (Gresho and Sani, 1998).

For the sensibility analysis, interest variables are post-processed after the solution of a EVP fluid flow for $Re_{pl} = 1$, $HB = 1$, $Wi = 1$, $Pa = 10000$, and $K* = 1$: dimensionless extra-stress magnitude τ^* and elastic strain γ_e are examined in the plate center (x^*_1 = 0.5 l) along x^*_2-direction. Locally, in a unyielded region over the plate both variables are evaluated. The sensibility analysis in the longitudinal direction is performed. A constant progression in longitudinal

direction in all meshes is considered, coarse to extra-fine, respectively $M1$, $M2$, $M3$, and $M4$. The refinement between meshes consider the ratio $1:2:4:6$, from $M1$ to $M4$ mesh. The minimum element mesh size in the longitudinal direction $h^*_{K\,min}(x^*_1)$ is equal to 593E-04 L to 3.029E-04 L, respectively $M1$ to $M4$.

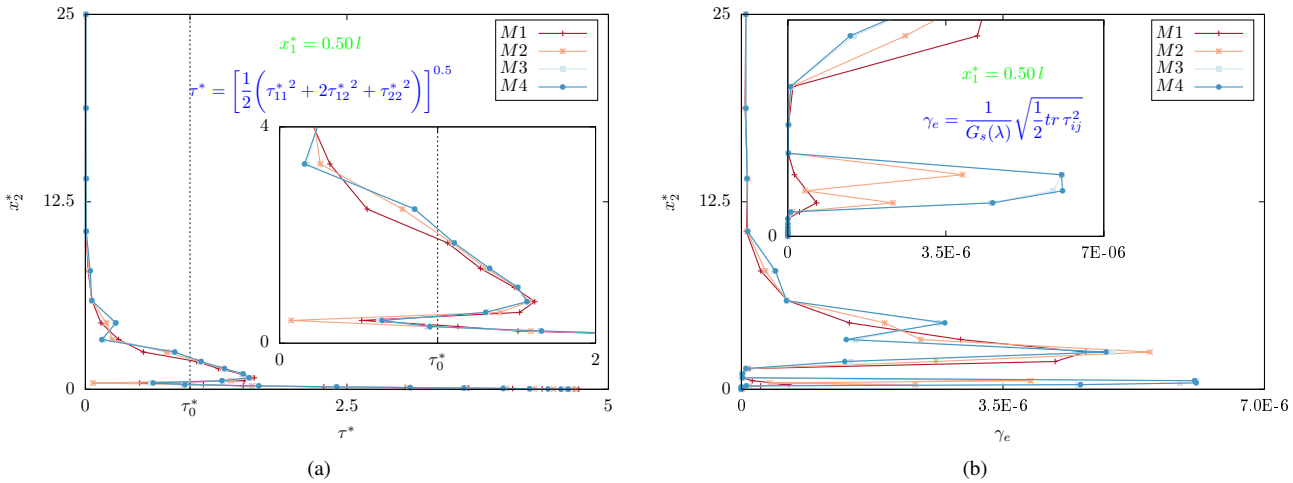

(a) (b)

Figure 5: Sensibility analysis: plots of (a) τ^* and (b) γ_e of base EVP fluid for $Re_{pl} = 1$, $HB = 1$, $Wi = 1$, $Pa = 10000$, and $K* = 1$.

As a local sensibility analysis, τ^* is evaluate. The relative percentage error (RPE) estimative $RPE(u) = (|u_n - u_{n+1}|/u_n)\,\mathrm{x}\,100$ is calculated. Tab. (1) show the structured EVP fluid sensitivity analysis of the parameter.

Table 1: Sensitivity analysis based in the RPE estimative of elastic strain.

Mesh	Number of elements	Number of degrees of freedom (DOF)	h^*_{kmin} (1E-04)	τ^*	RPE (%)
$M1$	1538	8850	593.09	0.51928	-
$M2$	2812	16050	16.61	0.7324	41.04
$M3$	6504	37350	5.31	0.62821	14.22
$M4$	9104	52350	3.02	0.64855	3.13

The problem shows error minimization issues due to the high non-linearity. From Tab. (1), the mesh $M3$ present the smaller RPE estimative. A transverse plot of τ^*, Fig. (5a), shows zero-stress zones on the free-flow region for all meshes and a high-stress zones near the blade surface that exhibits a concise behavior for all meshes. The most significant difference is in the unyielded region over the blade.

Inside this region a elastic dominance is observed, Fig. (5b), with a high γ_e modulus in that region, see detail. The region near the blade have zero-γ_e evidencing the breakdown of the microstructure, high elastic modulus, and viscous dominance in a shear stress dominant region. The γ_e is related with stress and elastic modulus. Fig. (6) shows the detail of the unyielded zones.

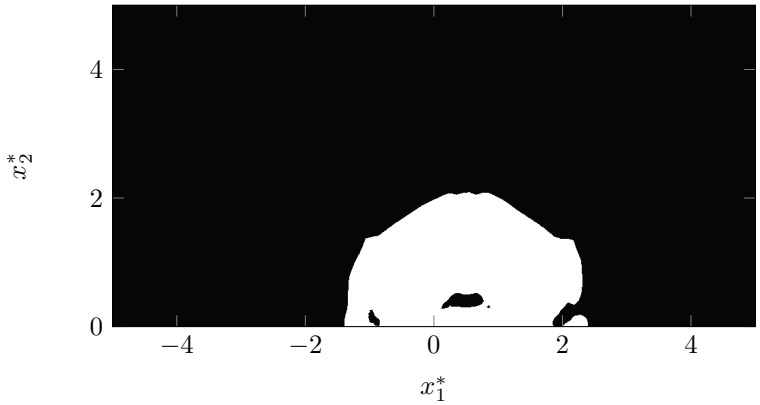

Figure 6: Detail of unyielded zones over the blade for base EVP fluid for $Re_{pl} = 1$, $HB = 1$, $Wi = 1$, $Pa = 10000$, and $K* = 1$. *The unyielded zones are colored in black.*

Although, the finite element method does not guarantee the local conservation of continuity, but the global one (**?**). It is then appropriated observe globally considering the mesh convergence. The root mean square percentage error (RMSPE) estimative based in the Sobolev norm is considered.

It is notice the constant RMSPE estimative on all studied meshes. Besides the ideal monotonical behavior, this characteristic indicates that all the meshes converge to the solution assuring global conservation of continuity, Fig. (**??**).

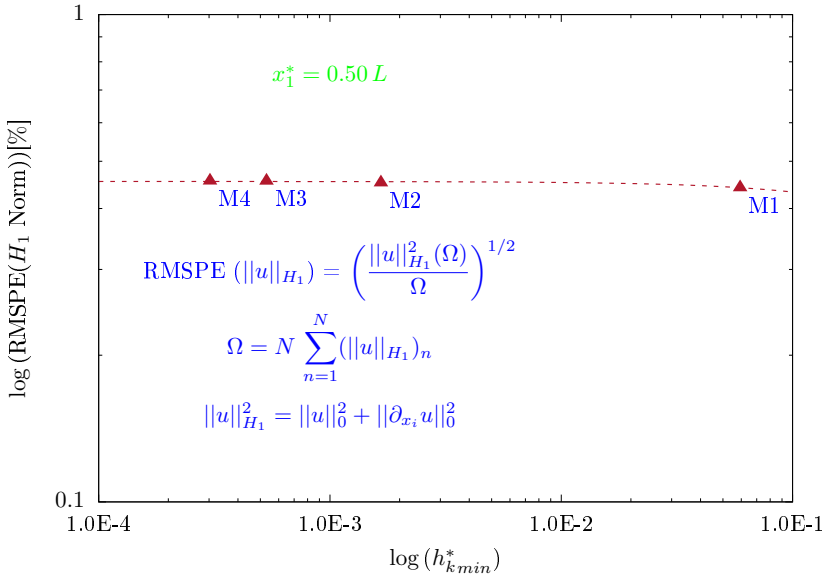

Figure 7: Sensibility analysis: log x log RMSPE Sobolev Norm and $h^*_{km} in$ of base EVP fluid for $Re_{pl} = 1$, $HB = 1$, $Wi = 1$, $Pa = 10000$, and $K* = 1$.

Considering the RPE and RMSPE estimative (with error above 1%) and the criteria of less computational effort (since to $M4$ is necessary 1E+10 memory positions for the solution of this type of problem), the mesh $M3$ is choosen.

5.3 Sensitivity of elastic parameter

The dimensionless positive parameter m relates the exponential elastic modulus and the microstructure level of the material. Eq. (9), shows this behavior and, in the dimensionless form, is given by:

$$G_s^*(\lambda) = G_0^* \exp\left[m\left(\frac{1}{\lambda} - 1\right)\right] \tag{15}$$

Eq. (15) is the dimensionless structural elastic modulus.

In the a fully unstructured flow region (e.g. in a polymer melt, the polymer chains are aligned with the flow direction and the viscous behavior is dominant), $G_s^*(\lambda \to 0) = 0$, and in a fully structured flow region (the polymer chains are entangle and the elastic behavior is dominant), $G_s^*(\lambda \to 1) = G_0^*$. The limit regions also mark the unyielded regions, where elasticity is dominant.

Between the limit regions Eq. (15) has an exponential behavior, where m is a factor that control the sensitivity of the transition region. For $m = 0$, $G_s^*(\lambda) = G_0^*$, Eq. (15) is independent of λ, the elastic behavior is dominant in All the flow regions. With the increase of m, the elastic dominanted regions shrink. The viscous dominance increase even for regions where the material is structured. For $m = 1$, $G_s^*(\lambda = 0.3) = 10.3\,G_0^*$, and for $m = 2$, $G_s^*(\lambda = 0.3)$ is multiply by a 10 factor.

The sensitivity of m takes place to evaluate correctly the unyielded regions without masking flow regions that originally must to be elastic dominated. Considering a base EVP material, Fig. (8) shows γ_e for various m values. For the increase of m, the γ_e maximum value decrease in the unyielded region above of the blade. The transition region, between the unyielded and yielded regions, is smoothened with the increase of m. For lower values of m near the blade, γ_e is increased due the higher ratio of τ^*/G_s^*, Eq. (15), where G_s^* tends to be constant and equals to G_0^* for $m \to 1$.

The τ^*, in the detail of Fig. (8), shows the unyielded and yielded regions for $\tau^* \leq \tau_0^*$ and $\tau^* > \tau_0^*$, respectively. The τ^* value is for $m = 5$. The m does not influence significantly the lenght of the unyielded regions. The unyielded region is smoothened with the decrease of m. In this work, considering the low- free-flow and high-rate of strain blade regions, the sensitivity elastic parameter $m = 5$ is choosen.

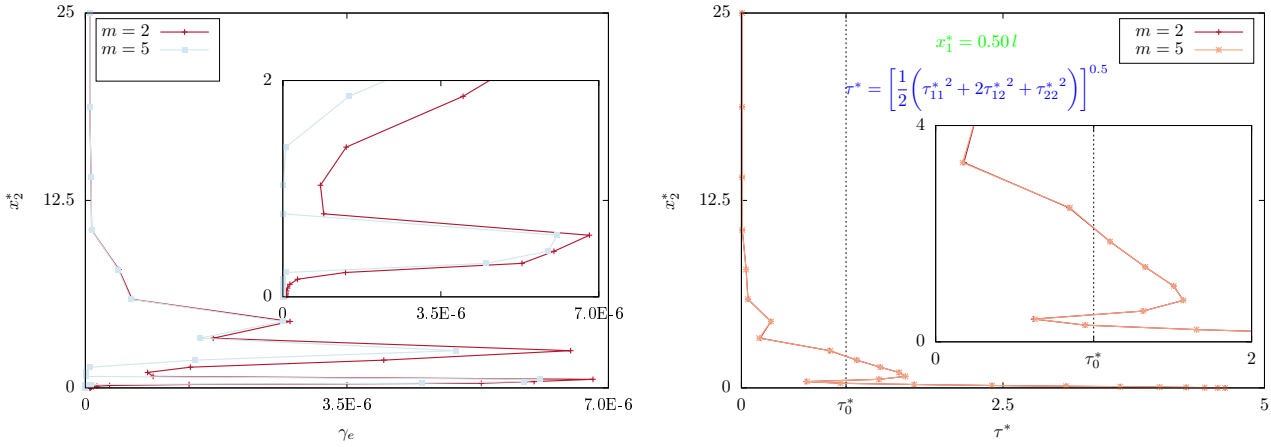

(a) (b)

Figure 8: Sensitivity of elastic parameter m for base EVP fluid for $Re_{pl} = 1$, $HB = 1$, $Wi = 1$, $Pa = 10000$, and $K* = 1$.

5.4 Sensitivity analysis

In this section the influence of the governing parameters is evaluated observing the unyielded zones. Initially, a special case of elasto-viscoplastic material is considered when the elastic and inertial presence are neglected, Fig. (9a). In this case the fluid could be considered as a inelastic and non-inertial viscoplastic material. It is possible notice a slightly symmetric unyielded zones considering the blade centerline at $x_1^* = 0.5\,l$. Besides neglecting the elastic and inertial presence, the microstruture level changes the pattern of the unyielded zones due to the shear stress in the blade.

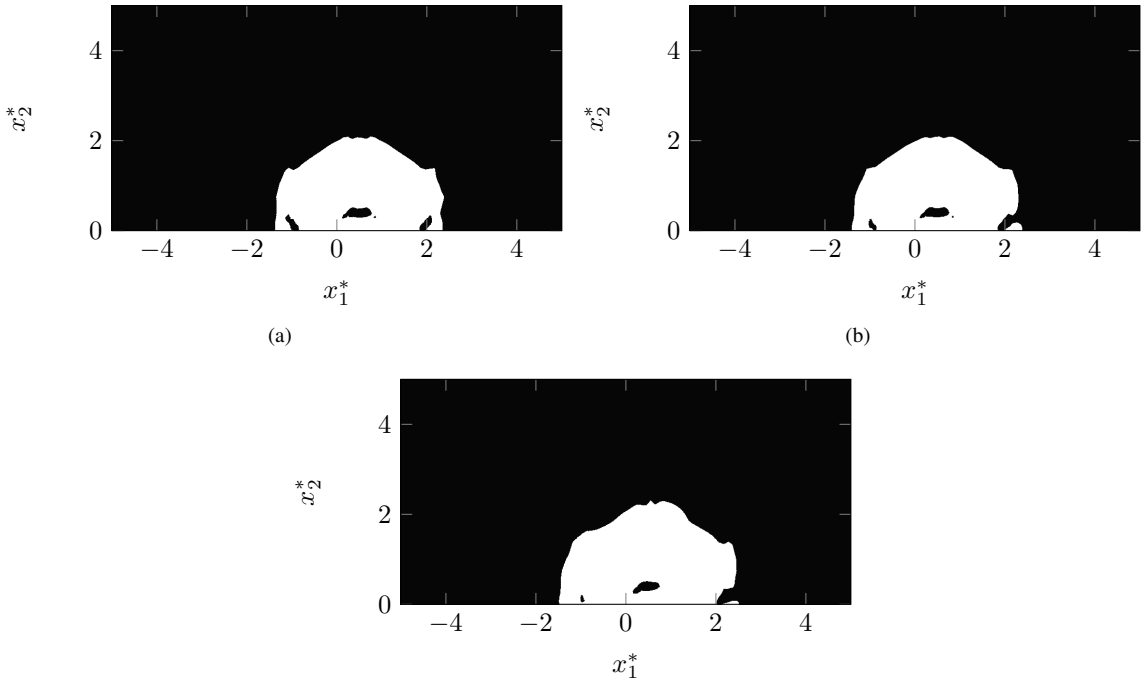

(a) (b)

(c)

Figure 9: Unyielded zones over the blade of VP material for (a) inelastic and non-inertial case ($Re_{pl} = 0$, $HB = 1$, $Wi = 0$, $Pa = 10000$, and $K^* = 1$), and base EVP material for $HB = 1$, $Wi = 1$, $Pa = 10000$, $K^* = 1$ evaluating the influence of power-law Reynolds: (b) $Re_{pl} = 1$, (c) $Re_{pl} = 10$. *The unyielded zones are colored in black.*

The elastic and inertial presence evidence the increase of elastic strain in the unyielded zones, Fig. (10). The increase of inertial effects characterized by the increasing power-law Reynolds show the reduction of elastic influence in previously high-elasto dominated regions.

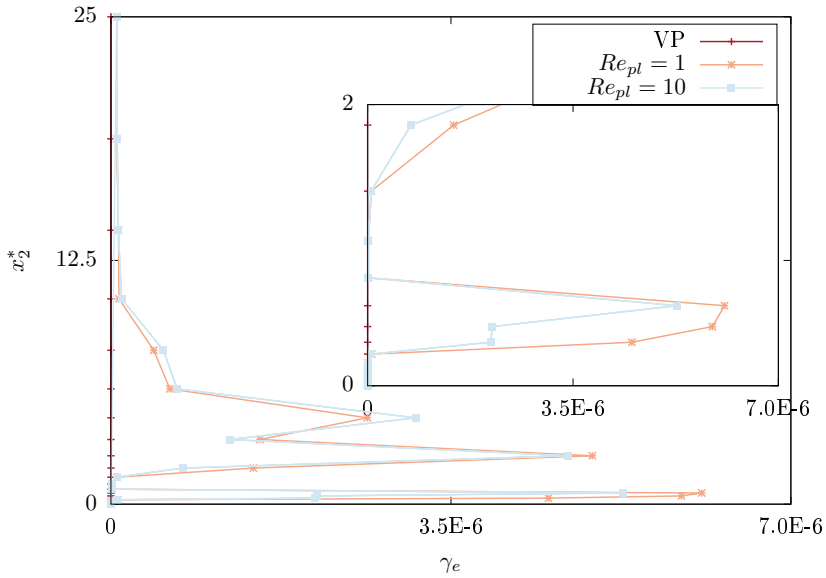

Figure 10: Elastic strain over the blade of VP and base EVP material: influence of power-law Reynolds.

6. CONCLUSION

This work focused in the approximated solution of a structured elasto-viscoplastic material via a three-field stabilized Galerkin least-square finite element method. The preliminary results show the interlace of the elastic parameter and elastic strain in the unyielded zones. Although the unyielded zones do not show relevant influence of the elastic parameter, the elastic dominance inside thoses zones have significant influence. Besides there are a strong relation between the inertial effects that expands and moves forward the unyielded zones over the blade in the flow direction.

7. ACKNOWLEDGEMENTS

The Authors would like to thank to Coordenação de Aperfeiçoamento de Pessoal de Nível Superior (CAPES) for the financial support.

8. REFERENCES

Acierno, D., La Mantia, F., Marrucci, G. and Titomanlio, G., 1976. "A non-linear viscoelastic model with structure-dependent relaxation times: I. basic formulation". *Journal of Non-Newtonian Fluid Mechanics*, Vol. 1, No. 2, pp. 125–146.

Behr, M.A., Franca, L.P. and Tezduyar, T.E., 1993a. "Stabilized finite element methods for the velocity-pressure-stress formulation of incompressible flows". *Comput. Methods Appl. Mech. Eng.*, Vol. 104, pp. 31–48.

Behr, M., Arora, D. and Pasquali, M., 2004. "Stabilized finite element methods of gls type for oldroyd-b viscoelastic fluid". *European Congress on Computational Methods in Applied Sciences and Engineering ECCOMAS*, pp. 24–28.

Behr, M.A., Franca, L.P. and Tezduyar, T.E., 1993b. "Stabilized finite element methods for the velocity-pressure-stress formulation of incompressible flows". *Computer Methods in Applied Mechanics and Engineering*, Vol. 104, No. 1, pp. 31–48.

de Souza Mendes, P.R., 2011. "Thixotropic elasto-viscoplastic model for structured fluids". *Soft Matter*, Vol. 7, No. 6, pp. 2471–2483.

de Souza Mendes, P.R. and Thompson, R.L., 2012. "A critical overview of elasto-viscoplastic thixotropic modeling". *Journal of Non-Newtonian Fluid Mechanics*, Vol. 187, pp. 8–15.

Fonseca, C., Frey, S., Naccache, M.F. and de Souza Mendes, P.R., 2013. "Flow of elasto-viscoplastic thixotropic liquids past a confined cylinder". *Journal of Non-Newtonian Fluid Mechanics*, Vol. 193, pp. 80–88.

Gresho, P.M. and Sani, R.L., 1998. "Incompressible flow and the finite element method. volume 1: Advection-diffusion and isothermal laminar flow".

Link, F.B., Frey, S., Thompson, R.L., Naccache, M.F. and de Souza Mendes, P.R., 2015. "Plane flow of thixotropic elasto-viscoplastic materials through a 1: 4 sudden expansion". *Journal of Non-Newtonian Fluid Mechanics*, Vol. 220, pp. 162–174.

Mendes, P.R.d.S., 2007. "Dimensionless non-Newtonian fluid mechanics". *J. Non-Newtonian Fluid Mech.*, Vol. 147, No. 1-2, pp. 109–116.

Mendes, P.R.d.S., 2011. "Thixotropic elasto-viscoplastic model for structured fluids". *Soft Matter*, Vol. 7, pp. 2471–2483.

Mendes, P.R.d.S. and Dutra, E.S.S., 2004. "Viscosity function for yield-stress liquids". *Applied Rheology*, Vol. 14, No. 6, pp. 296–302.

Oishi, C.M., Thompson, R.L. and Martins, F.P., 2016. "Transient motions of elasto-viscoplastic thixotropic materials subjected to an imposed stress field and to stress-based free-surface boundary conditions". *International Journal of Engineering Science*, Vol. 109, pp. 165–201.

Rajagopalan, D., Armstrong, R.C. and Brown, R.A., 1990. "Finite element methdos for calculation of steady, viscoelastic flow using constitutive equations with a newtonian viscosity". *Journal of Non-Newtonian Fluid Mechanics*, Vol. 36, pp. 159–192.

Zinani, F. and Frey, S., 2006. "Galerkin Least-Squares Finite Element Approximations for Isobaric Flows of Viscoplastic Liquids". *J. Fluids Engineering*, Vol. 128, pp. 853–863.

9. RESPONSIBILITY NOTICE

The authors are solely responsible for the printed material included in this paper.